



## Original Article

# The variant selection in the transformation from austenite to martensite in samples of maraging-350 steel

Neuman Fontenele Viana\*, Cristiana dos Santos Nunes,  
Hamilton Ferreira Gomes de Abreu

Universidade Federal do Ceará, Fortaleza, CE, Brazil

### ARTICLE INFO

#### Article history:

Received 19 February 2013

Accepted 25 March 2013

Available online 17 October 2013

#### Keywords:

Maraging steel

Martensite transformation

Variant selection

### ABSTRACT

Experiments have been conducted to study the variant selection phenomenon in the transformation from austenite to martensite in maraging-350 steel. The transformation of austenite to martensite in maraging steels occurs at temperatures below 300 °C depending on the alloy chemical composition. The transformation to martensite in these steels occurs regardless of the cooling rate. In these steels, the reverted austenite presents the same crystallographic texture of the mother austenite. Samples of maraging-350 were austenitized at 860 °C inside a furnace attached to a tension test machine and then cooled in the furnace until the temperature of 600 °C and 400 °C. At these temperatures samples were deformed by compression with 10% reduction in height. After deformation the applied force was removed and samples were cooled to room temperature in air. A second group of samples was subjected to the same austenitization and cooled until 300 °C when it was applied a compressive stress with magnitude below the yield strength. With the force applied, the samples were air cooled to room temperature. EBSD analysis was performed in cross-section of samples to determine the influence of plastic deformation before the transformation and also the influence of a stress in the elastic regime in the selection of variants of martensite. Measured pole figures were compared with calculated ones using the phenomenological martensite transformation concept associated with Patel–Cohen model.

© 2013 Brazilian Metallurgical, Materials and Mining Association. Published by Elsevier Editora Ltda. All rights reserved.

## 1. Introduction

Maraging steels belong to a family of carbon free iron–nickel alloys with additions of cobalt, molybdenum, titanium and aluminum. The term maraging is derived from the strengthening mechanism. Mar from martensite + aging means that the

alloy transforms to martensite with subsequent age hardening. This family of steels finds important applications where ultra-high strength is required, along with good dimensional stability during heat treatment [1].

The transformation of austenite to martensite in maraging steels occurs regardless of the cooling rate. The  $A_s$ ,  $A_f$ ,  $M_s$  and  $M_f$  temperatures were measured for the MAR350 cold

\* Corresponding author.

E-mail: [neumanfv@gmail.com](mailto:neumanfv@gmail.com) (N.F. Viana).

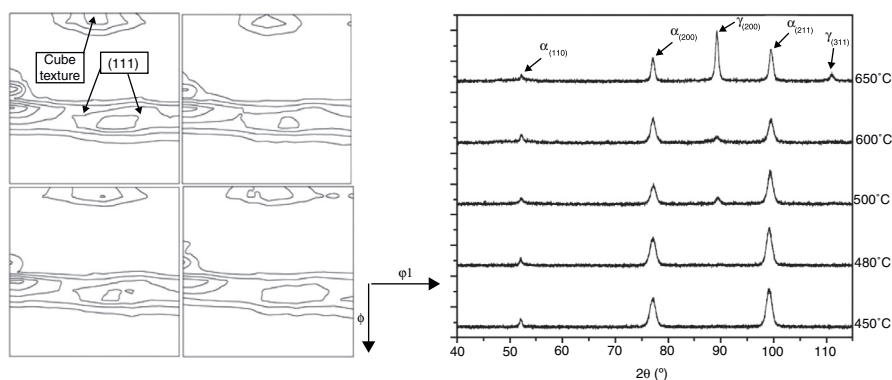


**Fig. 1 – (a)  $\varphi_2 = 45^\circ$  odf sections; (b) X-ray diffractograms for the martensite phase of samples aged at 450 °C, 480 °C, 500 °C and 650 °C.**

deformed 80% using thermo-magnetic analysis. The temperatures were found to be 690 °C, 800 °C, 175 °C and 130 °C, respectively [1].

Nakada et al. have studied the reversion of austenite in a martensitic stainless steel and concluded that most of reverted austenite had the same orientation as the original austenite matrix before martensitic transformation. They also suggested that reverted austenite retained a Kurdjumov–Sachs relationship to martensite [2].

The theory concerned with martensite transformation is well established. The crystallography of each plate of martensite can be described in terms of a mathematically connected set consisting of the habit plane, orientation relationship with the austenite, and the shape deformation [3–7].

The Patel and Cohen model for predicting the variant selection phenomenon is based in the energy of applied stress during transformation. The interaction energy that provides the mechanical driving force for transformation is given by Eq. (1) [8]:

$$U = \sigma_N \zeta + \tau s \quad (1)$$

where  $\sigma_N$  is the stress component normal to the habit plane,  $\tau$  is the shear stress resolved on the habit plane in the direction of shear  $\alpha$ ,  $\zeta$  and  $s$  are respectively normal and shear strains associated with transformation [3]. The total free energy available for transformation is the sum of chemical and mechanical components, according to Eq. (2); the latter one being zero in the absence of an applied stress during transformation [4]:

$$\Delta G = \Delta G_{CHEM} + \Delta G_{MECH} \quad (2)$$

where  $\Delta G_{MECH} \equiv U$ . It would be reasonable to assume that there is strong variant selection when the ratio of  $\Delta G_{MECH}/\Delta G$  is large [4].

In this work, samples of maraging 350 were austenitized at 860 °C inside a furnace attached to a tension test machine and then cooled in the furnace until the temperature of 600 °C and 400 °C. At this temperature the samples were deformed by compression with reductions in height below 10%. After deformation the force was removed and samples were cooled to room temperature. A second group of samples was subjected to the same austenitization and cooled to 300 °C when

it was applied a compressive stress with magnitude below the yield strength. With the force applied, the samples were air cooled to room temperature. Pole figures obtained by EBSD were compared with calculated pole figures based on the phenomenological martensite transformation crystallography (PMTC) associated to the Patel–Cohen model.

## 2. Experimental

Samples of forged MAR350 steel with the composition 19.77 Ni, 10.74 Co, 4.70 Mo, 1.4 Ti, 0.10 Al, 0.0073 C and balance of Fe were austenitized at 860 °C for 1 h and cooled inside a furnace assembled to a Universal testing machine. When the temperature reached 600 °C and 400 °C samples were pressed resulting in a 10% of plastic deformation. Another sample was cooled to 300 °C when a compressive stress of 200 MPa – below the yielding of Mar 350 at this temperature – was applied and kept until the end of transformation. To find the orientation of the previous austenite, samples were aged at 550 °C for 1 h to precipitate reverted austenite.

The EBSD study was performed in an Oxford Channel 5-EBSD system attached to a SEM Philips XL-30. Sample preparation sequence was a pre-grind to 600 SiC and polish to 3- $\mu$ m diamond. The final polishing was done using a colloidal silica suspension of particle size of 0.05  $\mu$ m during long periods of time. X-ray diffraction was performed in a Philips diffractometer model X'Pert Pro using Co K $\alpha$  radiation with an attached monochromator.

To reproduce the phenomenological theory of martensite transformation crystallography the software crystal.habit.poly.f. Details of use of this software are available in Ref. [9].

## 3. Results

The first task of this work was to assure that the reverted and the parent austenite presented the same crystallographic texture. Fig. 1a shows  $\varphi_2 = 45^\circ$  odf (orientation distribution functions) sections for the martensite phase of samples aged at 450 °C, 480 °C, 500 °C and 650 °C. Comparing odf's, it can be noted that main components of texture for the four aged

conditions are a cube component  $(001)[100]$  and the  $(111)$  fiber more intense in  $\{111\}(112)$ . Samples aged at  $500^\circ\text{C}$  and  $650^\circ\text{C}$  shows peaks of reverted austenite on the diffractogram presented in Fig. 1b and no change in the crystallographic texture of the martensite phase.

Fig. 2 shows EBSD maps for martensite and austenite for a sample of maraging aged for 1 h at  $550^\circ\text{C}$  and cooled in air without stress or prior deformation before martensite transformation. The color of each point is associated to the local orientation, as shown in the orientation standard triangle. The selected grain for study is the one in blue in the central part of Fig. 2b.

The orientation of austenite in the selected grain was determined by the EBSD Channel 5 software and is represented by the set of Euler angles  $-\varphi_1 = 334.3^\circ$ ,  $\phi = 47.9^\circ$  and  $\varphi_2 = 60.3^\circ$ . To perform the calculation of orientation of the martensite resulting from the transformation, a complete set of crystallographic data is necessary. Unfortunately, such data for maraging steel is not available. A data that corresponds to the traditional twinned  $\{259\}_\gamma$  transformation found in high carbon steels, Fe-Ni and Fe-Ni-C will be used [10-12].

The choice of lattice invariant shear (LIS) was the  $(112)[111]_\alpha$  twinning system in the bcc phase, that corresponds to  $(111)[101]_\gamma$  in the fcc phase.

The following data was obtained:

Magnitude of LIS ' $g$ ' = 0.272602.

Magnitude of the shape strain ' $m$ ' = 0.219957.

Habit plane:

$(-0.416781 \ 0.588617 \ 0.694388)_\alpha$

or

$(0.185064 \ 0.594242 \ -0.782705)_\gamma$

Shape strain direction:

$[0.628457 \ -0.478456 \ 0.613288]_\alpha$

or

$[0.209536 \ 0.672823 \ 0.709509]_\gamma$

Orientation relationship:

$[100]_\gamma = [0.723985 \ 0.677740 \ 0.128506]_\alpha$

$[010]_\gamma = [-0.018574 \ -0.167069 \ 0.985770]_\alpha$

$[001]_\gamma = [0.689565 \ -0.716070 \ -0.108367]_\alpha$

Fig. 3a shows  $(100)$  calculated pole figure for martensite using the phenomenological martensite transformation crystallography theory and assuming that all 24 variants are present, i.e., no variant selection is acting. It was compared with measured  $(100)$  bcc pole figure for the same region and is presented in Fig. 3b. There is a very good match between calculated and measured pole figures. These result points to the fact that reverted and parent austenite have the same crystallographic texture. It is also evident that there is no variant selection in this transformation.

Fig. 4 shows the contrast map of a cross-sectional area of the specimen deformed 10% at its height in a compression test performed at  $400^\circ\text{C}$ . The circle marked in the figure indicates the austenite grain used to study the crystallography of the transformation.

Fig. 5 compares  $(100)$  calculated pole figure in (a) and (b) with one measured by EBSD in one grain that belongs to a sample deformed 10% in its height by the application of a compressive force at  $400^\circ\text{C}$ , i.e., before martensite transformation. In Fig. 5a it was assumed that there was no variant selection. In Fig. 5b, it was assumed that some vestige of

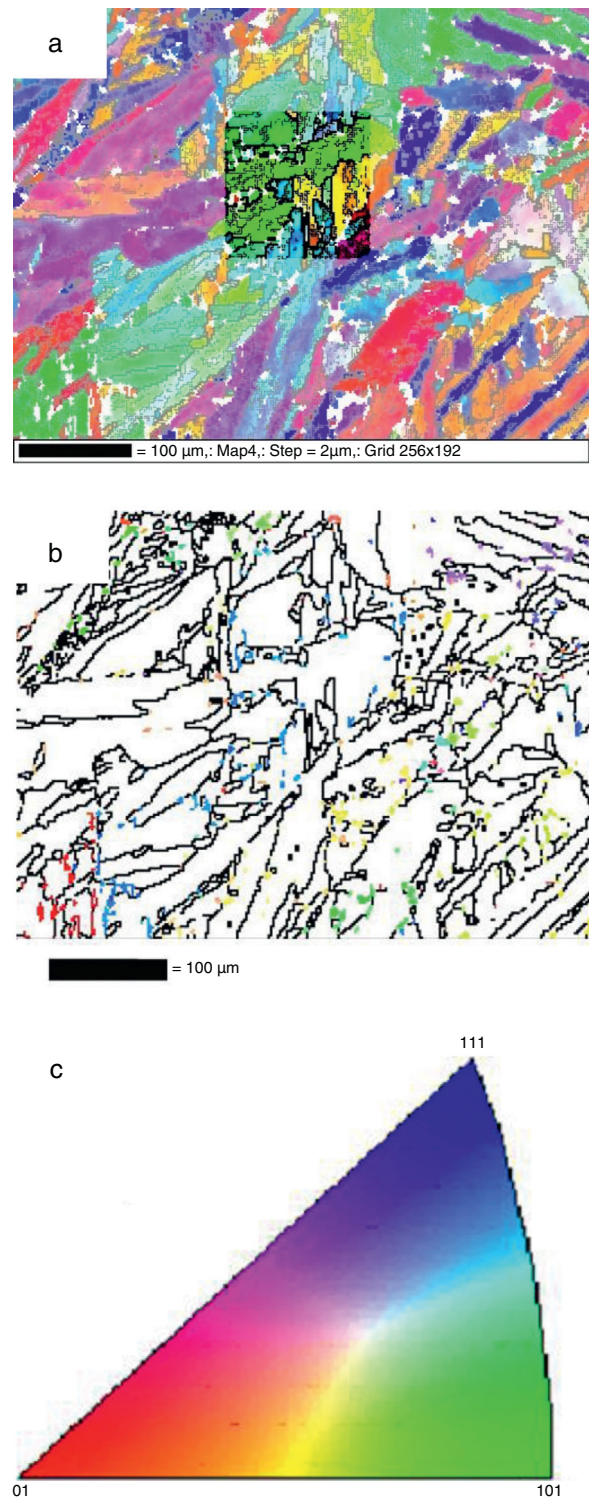


Fig. 2 - (a) EBSD map for martensite; (b) EBSD map for austenite; (c) standard triangle. (For interpretation of color in the text, the reader is referred to the web version of the article.)

the original applied stress was influencing the variant selection phenomenon and only 10 variants with higher values of mechanical energy are present. Comparing Fig. 5a-c it can be seen that all variants found in the measured pole figure of the sample were provided by PMTC. Making the same



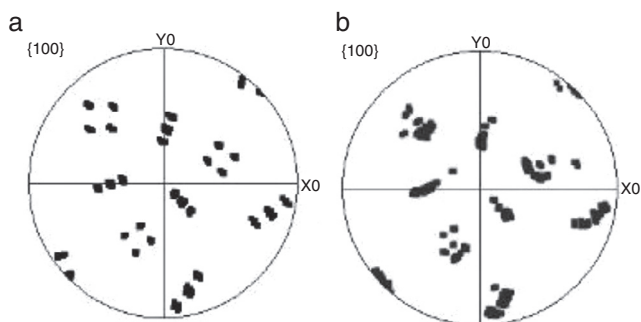


Fig. 3 – Calculated (a) and measured (b) (100) pole figures for bcc phase in area shown in Fig. 2c.

comparison with the pole figure calculated assuming the model of Patel–Cohen one realizes that variants not predicted by the model appeared as well as variants predicted by the model are not present. The probable reason for the divergence is that after withdrawing the force that made plastic deformation in the sample, it was placed in air for cooling and during cooling thermal stresses arose influencing the variant selection process.

For the sample deformed at 600 °C the same phenomenon happened. All variants predicted by the PMTC assuming 24 variants are present in Fig. 6c. Some variants with positive mechanical energy predicted by the Patel–Cohen model are present and some not. There are also variants not predicted by the model that precipitated.

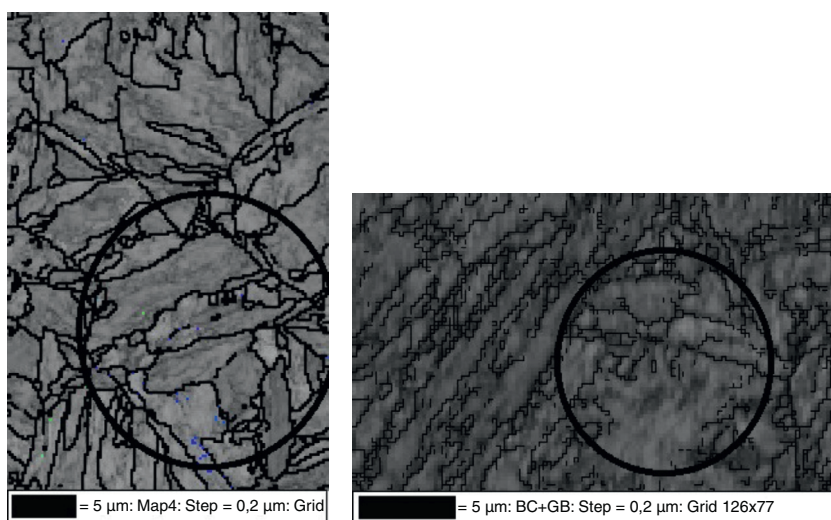


Fig. 4 – Contrast map of the sample deformed at 400 °C and at 600 °C.

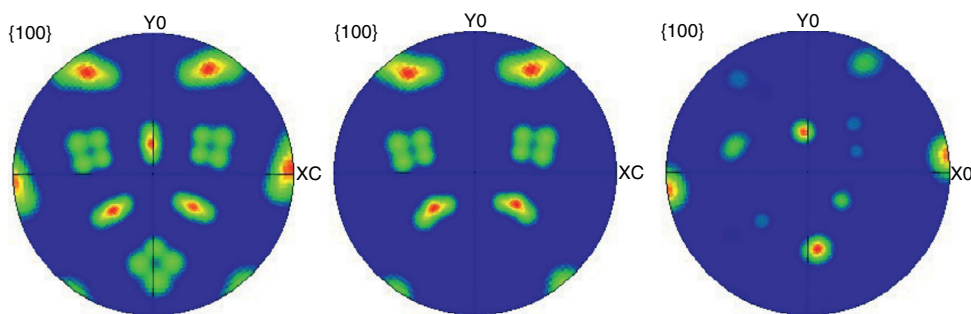


Fig. 5 – (100) pole figures for a sample deformed at 400 °C before transformation: (a) calculated 24 variants; (b) calculated 9 variants; (c) measured.

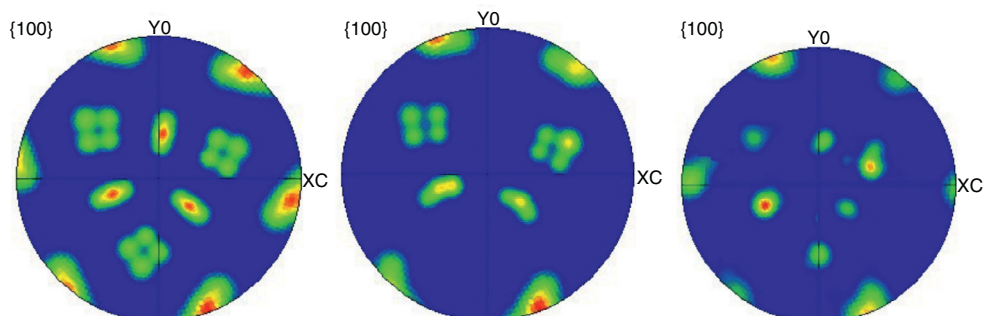
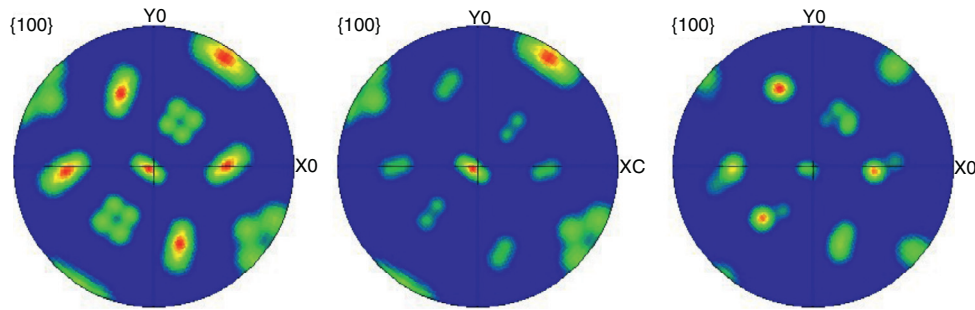


Fig. 6 – (100) pole figures for a sample deformed at 600 °C before transformation: (a) calculated 24 variants; (b) calculated 9 variants; (c) measured.



**Fig. 7 – {100} pole figures for a sample with elastic applied stress during transformation: (a) calculated 24 variants; (b) calculated 12 variants; (c) measured.**

Finally the last sample was not plastically deformed before martensitic transformation is shown in Fig. 7. This sample showed a very good match between calculated pole figure and measured pole figure. The Patel and Cohen model was developed to analyze the influence of stress during transformation. This sample was not subject to any plastic deformation before martensitic transformation only elastic compressive stress at the transformation temperature.

#### 4. Summary

The phenomenological theory of martensite crystallography (PMTTC) showed to be very accurate to simulate transformation texture in maraging-350 steel. The Patel and Cohen criterion was very precise for predicting variant selection in samples where transformation took place under the action of an external stress. Samples plastically deformed in temperatures above  $M_s$  presented a variant selection different than the predicted by the model.

#### Conflicts of interest

The authors declare no conflicts of interest.

#### Acknowledgements

The authors are grateful to the support from CNPq (National Council for Scientific and Technological Development) projects 304503/2011-8 and 475825/2011-0.

#### REFERENCES

- [1] Tavares SSM, Abreu HFG, Neto JM, da Silva MR, Popa I. A thermomagnetic study of the martensite–austenite phase transition in the maraging 350 steel. *J Alloys Compd* 2003;358:152–6.
- [2] Nakada N, Tsuchiyama T, Takaki S, Hashizume S. Variant selection of reversed austenite in lath martensite. *ISIJ Int* 2007;47:1527–32.
- [3] Kundu S, Bhadeshia HKDK. Crystallographic texture and intervening transformations. *Scr Mater* 2007;57: 869–72.
- [4] Kundu S, Bhadeshia HKDK. Transformation texture in deformed stainless steel. *Scr Mater* 2006;55: 779–81.
- [5] Bowles JS, MacKenzie JK. The crystallography of martensite transformations. *Acta Metall* 1954;2:129–37.
- [6] MacKenzie JK, Bowles JS. The crystallography of martensite transformations II. *Acta Metall* 1954;2:138–47.
- [7] Bhadeshia HKDK. *Geometry of crystals*. 2nd ed. London: Institute of Materials; 2001.
- [8] Patel JR, Cohen M. Criterion for the action of applied stress in the martensitic transformation. *Acta Mater* 1953;1: 531–8.
- [9] Kundu S. University of Cambridge; 2007. Available from: [www.msm.cam.ac.uk/phasetrans/](http://www.msm.cam.ac.uk/phasetrans/) [PhD thesis].
- [10] Bowden HG, Kelly PM. The crystallography of the pressure induced phase transformations in iron alloys. *Acta Metall* 1967;15:1489–500.
- [11] Kelly PM. *ISI Special Rep* 1964;86:146.
- [12] Kelly PM. The martensite transformation in steels with low stacking fault energy. *Acta Metall* 1965;13:635–46.